Optimization of Multi-Pump Raman Amplifiers

André Richter, Igor Koltchanov
VPIphotonics (a division of VPIsystems), Carnotstrasse. 6, D-10587 Berlin, Germany
andre.richter@vpiphotonics.com

Eugene Myslivets, Anatoliy Khilo, Gena Shkred
VPI Development Center, 220034 Minsk, Belarus

Ronald Freund
Fraunhofer Institute for Telecommunications, Heinrich-Hertz-Institut, Einsteinufer 37, 10587 Berlin, Germany

Introduction

The utilization of high-gain bandwidth in fiber Raman amplifiers (FRA) requires multiple pumps at different wavelengths and careful adjustment of the individual pump powers [1-2]. Due to the large number of varying, partly unknown parameters, this is only feasible with the help of special optimization algorithms [3-4]. It is essential that such optimization routines consider pump-pump and pump-signal Raman interactions. However, other physical effects, whose impact is a priori unknown within the scope of the optimizer, can have a significant influence on the performance of the Raman amplifier. For instance, signal-signal Raman interactions, Rayleigh and Brillouin scattering, and power-related variations of broadband pump sources can cause considerable amplifier degradations. Therefore, it is essential that those effects are considered carefully and that realistic fiber and component characteristics are used to obtain meaningful optimization results.

In this paper, we present a new technique for automatic optimization of multi-pump Raman amplifiers complying with the constraints listed above while keeping the simulation time within reasonable limits. Our multi-step approach considers first, fiber attenuation and interactions between WDM signals and Raman pumps, and then, any other effects by treating them as external perturbation in an iterative process. Results of pump optimizations are shown demonstrating how various physical effects can influence the design of multi-pump FRAs.

Optimization technique

At first, the algorithm adjusts the pump powers for given nominal pump wavelengths to obtain any desirable gain spectrum defined by pump-pump and pump-signal interactions alone. For this, the algorithm uses the fiber length, wavelength-dependent attenuation, core area and Raman gain profiles as input. Raman pumps are assumed to be monochromatic for now. As discussed in [3-4], the fiber propagation function $T(f)$ in dB units can be represented as a sum of the partial Raman contributions $G_k(f)$ from each of M pumps and the total loss $L(f)$:

$$T(f) = \sum_{k=1}^{M} G_k(f)\overline{P}_k - L(f) \to \tilde{T}(f) \qquad (1)$$

where $\overline{P}_k$ are the path-averaged pump powers, which are optimized so that the resulting transfer function deviates as little as possible from the goal function $\tilde{T}(f)$ while holding all constraints. The optimization task (1) can be solved numerically without much effort allowing the optimum launch pump powers P_k to be found after a few iterations by adjusting their levels so that the path-averaged powers match the required values. Considered constraints of the optimization task are, for instance

$$\overline{P}_k \geq 0, \quad \sum_{k=1}^{M} P_k \geq P_{total}, \quad P_{\min} \geq P_k \geq P_{\max}.$$

In the second optimization step, the Raman tilt caused by signal-signal interactions and any other power-related effects in the fiber link (such as Brillouin and Rayleigh scattering, splice loss/reflection, etc.) are accounted for as external perturbations $\Delta T(f)$ to $\tilde{T}(f)$ in (1). Resetting the goal function in (1) to $\tilde{T}(f) - \Delta T(f)$ results in perfect compensation of the perturbations $\Delta T(f)$. As $\Delta T(f)$ depends on the pumping power and is a priori unknown, it is calculated in an iterative process by comparing the transfer function calculated with (1) and the actual transfer function obtained in a numerical fiber simulation, which includes all perturbation effects [5]. For the case that the transfer function calculated in (1) converges with the actual transfer function, the estimated correction of the goal function approaches the exact value, and the whole optimization task delivers a self-consistent solution. The Raman

optimization algorithm was implemented in the photonic design environment of VPItransmissionMaker™ and tested for various application cases.

Several design examples are presented in the following. First, results from Raman pump optimization over a heterogeneous fiber span are demonstrated. Then, the impact of Rayleigh and Brillouin scattering on the gain and noise characteristics of FRAs is investigated. Finally, it is demonstrated that power-related variations of broadband pump sources can have a significant influence on the optimization results.

Pumping of heterogeneous fiber spans

The following shows the optimization of bidirectional pumped Raman amplification over a span containing three sections of fiber for dispersion management. The first and third sections consist of super large effective area fibers (SLA) of 35.45 km length, while the middle section is an inverse dispersion fiber (IDF) of 29.1 km length [6]. The splice loss between the sections is assumed to be 0.15 dB. Five Raman pumps are used: two in forward direction (1431 nm, 1466 nm), and three in backward direction (1424 nm, 1445 nm, 1452 nm). The optimization is based around a universal fiber model [5] that can represent heterogeneous fiber spans in a single module for computational efficiency. 40 test channels at wavelengths between 1530 and 1561 nm are sent into the heterogeneous fiber span. The target gain of the Raman optimizer is set to compensate all channels for the accumulated fiber attenuation under the constraint that the found pump powers are between 50 and 350 mW.

Figure 1 shows the pumping configuration and the found signal power distribution of the 40 test channels along the fiber for optimized pump powers. The maximum gain ripple at the output of the fiber was approximately 0.5 dB. The maximum difference of the optical signal-to-noise ratio (OSNR) between the 40 channels was approximately 1 dB. When increasing the number of pumps, smaller gain and OSNR ripples can easily be achieved as the optimum Raman pump power profile is better fitted by pumps at the given wavelengths. The signal power distribution shows clearly the wavelength dependence of the Raman gain along the heterogeneous fiber span. Note that considering the two splices correctly is vital to correct modeling of the Raman amplifier performance.

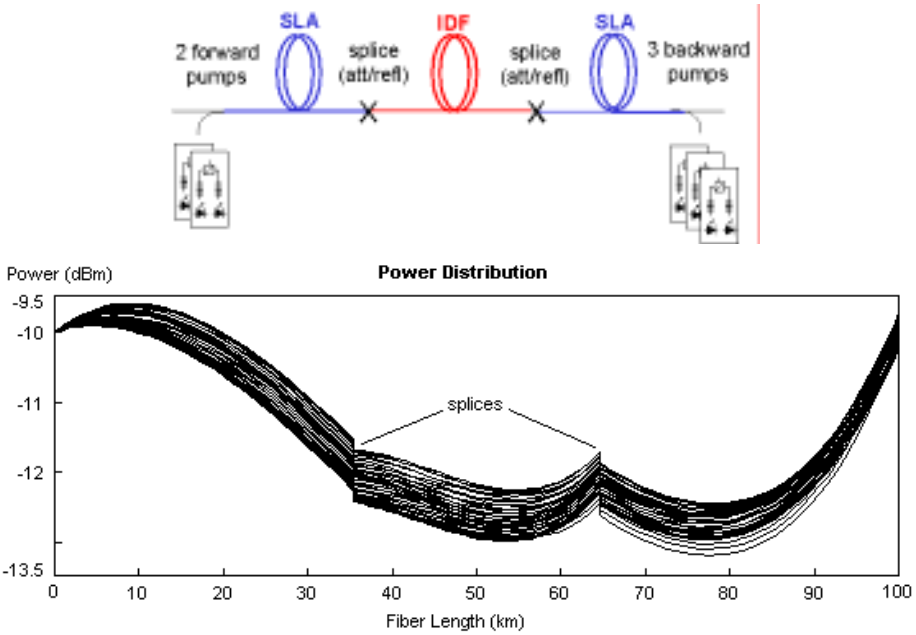

Fig. 1 Raman optimization over heterogeneous fiber spans for bidirectional Raman pumping; top: three-section fiber and Raman pumps; bottom: signal power distribution along the fiber.

Influence of Rayleigh and Brillouin scattering

It has been shown that Rayleigh scattering (RS) and stimulated Brillouin scattering (SBS) can cause considerable amplifier degradations [7-10]. Here we report results of pump optimizations demonstrating that these effects play a significant role and must not be ignored when designing multi-pump FRAs. The discrete FRA we optimized resembles the one in [2]. It consisted of 25 km non-zero dispersion shifted fiber (NZ-DSF), which was pumped in the backward direction at 12 wavelengths (1413 - 1504 nm) to provide 10.5 dB net gain for 100 WDM channels

(1527 - 1607 nm). Optimizations were carried out for the high and low signal power condition, e.g., signal powers of 0 and –10 dBm, respectively.

In a first step, we evaluated the Raman optimization process neglecting SBS and RS, but including Raman pump depletion and tilt due to signal-signal interactions. The additional tilt $-\Delta T(\lambda)$, which was added to the goal function of the pump-signal Raman gain in order to compensate the signal-signal interactions, was 7 and 1.2 dB for high and low signal condition, respectively, and thus non-negligible (Figure 2).

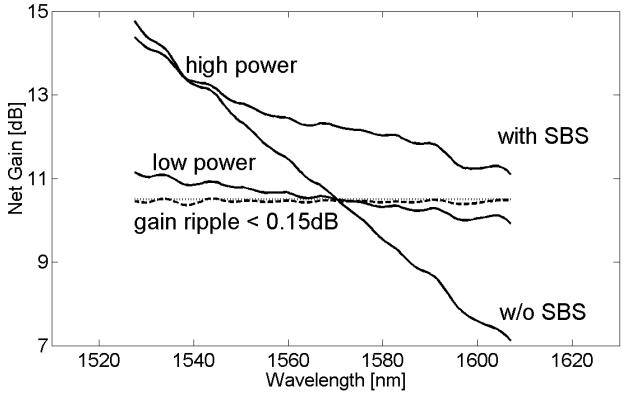

Fig. 2 Optimized Raman gains. Dotted curve: target gain, dashed curve: optimized Raman gain, solid curves: pump-signal Raman gain including the compensation $-\Delta T(\lambda)$ for signal-signal interactions, stimulated Brillouin scattering and Rayleigh scattering.

In a second step, we added Rayleigh scattering, representing an application case where SBS was suppressed. As shown in Figure 3 (left), the amplified spontaneous Raman scattering (ASRS) varied between -38.4 dBm (short wavelengths) and -41.4 dBm (long wavelengths), and thus, showed a typical tilt for backward-pumped amplifiers [11]. We found for both signal levels that RS of the WDM channels and pumps did not disturb the reference tuning of the amplifier. However, it is well known that double RS may be detrimental as the resulting multi-path interferences (MPI) decrease the total OSNR [7-8]. The MPI level was –43 dBm in the considered wavelength range for the high signal condition, and thus, comparable to the ASRS level. For the low signal condition, the MPI level was 10 dB below the ASRS level, and thus, negligible.

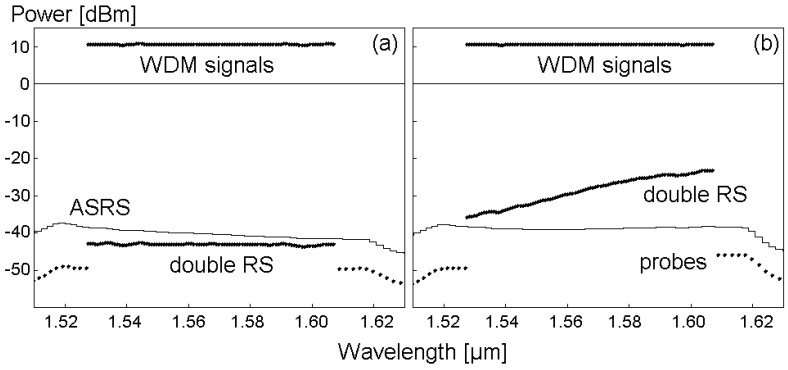

Fig. 3 Optical spectrum at the FRA output without SBS (a) and with SBS (b). Amplified Spontaneous Raman Scattering (ASRS) measured over 0.1 nm.

In a third step, we added the SBS effect. Due to their larger power, the pumps are much more liable to SBS than the signals. Hence, it is mandatory to suppress SBS for the Raman pumps as much as possible. We assumed that SBS for the pumps is fully suppressed as in [9-10]. For the low signal condition, amplifier operation has not changed significantly when SBS is added. For the high signal condition however, it has changed dramatically. The SBS reflection of the WDM signals causes additional losses, predominantly for the long wavelengths. While the net Raman gain accumulated over the whole FRA length is balanced for different channels, the spatial distributions of the short- and long-wavelength signals are different (Figure 4). The path-averaged power of the long-wavelength channels is higher, which causes stronger SBS.

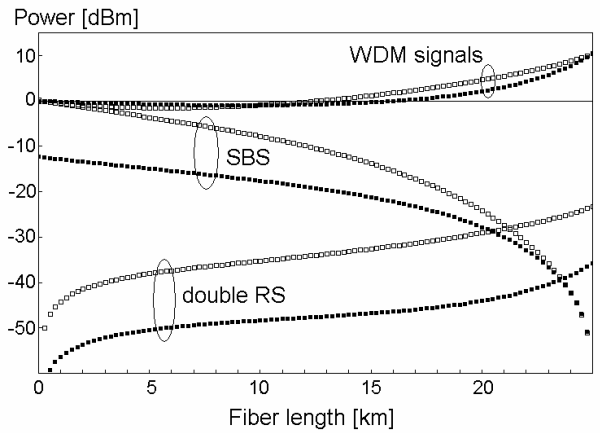

Fig. 4 Power profile of signals and distortions along the FRA.
Open symbols: long signal wavelength; closed symbols: short signal wavelength.

Without re-adjustment of the pump powers, the SBS effect led to ~1.3 dB tilt of the net FRA gain. Figure 5 shows the re-adjusted pump powers as automatically found by our optimizer. They mainly increased the contribution of the pump-signal Raman gain for the long wavelengths (Figure 2). The amount of gain required for the compensation of SBS was ~4 dB, which is larger than the mentioned 1.3 dB because of the fast increase of SBS strength with signal power.

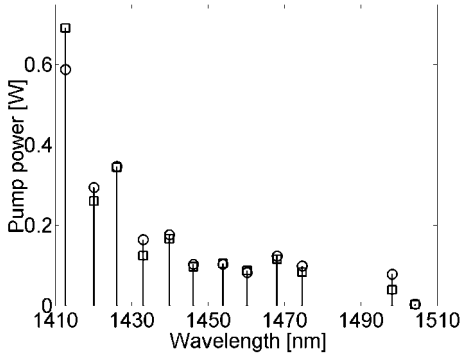

Fig. 5 Optimized pump powers without considering SBS (circles)
and with considering SBS (squares).

Unlike the WDM signals, Rayleigh distortions did not suffer substantially from SBS loss due to their small power, however, they were amplified as the WDM signals by the re-adjusted pumps. This led to a dramatically increased MPI level of -35.7 and –23.0 dBm for the short and long wavelengths respectively. Figure 3 shows that the ASRS tilt is flattened by the opposite SBS-induced tilt. The high MPI level results in a strong increase of the effective noise figure (NF) of the FRA. Figure 6 shows the on-off Gain and NF for the different cases that were investigated. To measure the gain and NF outside the WDM signal range, we added additional probes with input powers of –60 dBm (Figure 3). Due to their small powers, the probes are not subject to SBS losses and generate negligible double RS terms. Consequently, the net gain is higher (and the NF lower) for the probes than for WDM signals if placed at the same wavelengths. This explains the discontinuities of gain and NF at the boundaries of the WDM signal range in Figure 6.

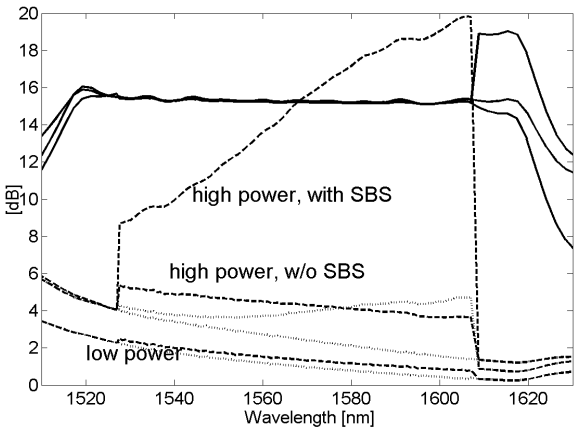

Fig. 6 Raman gain and noise figures. Solid curves: net Raman gains; dotted curves: noise figures; dashed curves: noise figures including MPIs.

The strong dependence of SBS that was observed is consistent with [9-10] where it was shown that the SBS threshold significantly decreases in Raman pumped fibers. Hence, optimized Raman pump powers that are found when ignoring SBS might not be accurate enough when operating under a high signal power condition, where SBS needs to be considered.

Power-related variations of broadband pump sources

Pump linewidth broadening and drift at high powers can have a significant influence when optimizing multi-pump Raman amplifiers. The power supplied by a high-power laser source is typically pumped over several nm's into the fiber. When adjusting the laser currents to control the total pump power, quite significant spectral changes of broadband pump sources can be observed. We demonstrate the influence of these variations when designing multi-pump Raman amplified systems.

It has been outlined above how the optimized Raman gain can be found for monochromatic pump sources. To consider the actual spectral shapes of broadband pumps in the optimization, a third sub-optimization step has been added. A single Raman gain function was used for the first two steps that has been measured using a monochromatic pump source. Proper frequency scaling [5] was applied before utilizing it to calculate the Raman contribution of each pump at any signal frequency. In the additional third step, an individual Raman gain function is calculated for each broadband pump g_R^b by convolving the Raman gain function of the monochromatic pumping case g_R^{mc} with the spectral shape of each pump:

$$g_R^b(f_p, \Delta f, P_t) = \int P_p(f, P_t) \cdot g_R^{mc}(f, \Delta f - f + f_p) df \qquad (2)$$

where P_p is the frequency-resolved pump power for a given total pump power P_t at the nominal pump frequency f_p. Those adaptations are considered for as external perturbations to the solution found in step two, which are compensated for by iteratively resetting the goal function of step two. As the pump spectra are power dependent, g_R^b needs to be recalculated for all iterations.

To demonstrate its application, we optimized the power of nine backward-pumped laser diodes into 80 km standard single-mode fibers (S-SMF) such that their induced Raman gain compensates completely the fiber loss over a bandwidth of 75 WDM channels (1540 - 1600 nm). To test the limits of our algorithm, the selected laser diodes were not wavelength-stabilized (using, e.g., an external fiber Bragg-grating). This scenario corresponds to the case where cheap, small and robust pumping solutions are required (such as in metro WDM applications). The nominal wavelengths of the diodes are between 1428 and 1496 nm. The total pump power per diode could be adjusted between 10 and 200 mW. Figure 7 (a) shows the measured spectrum of the 1470 nm diode for different pump currents. It demonstrates clearly the power-related spectral variations of the sources we have used here. This variation of the pump spectrum is translated into variations of the Raman gain coefficient g_R^b (as shown in Figure 7 (b)). The information of fiber attenuation and core area versus wavelength that we used in our simulations has been obtained from data sheets [12], while the wavelength-dependent Raman gain coefficient has been obtained from measurements performed by the NIST [13].

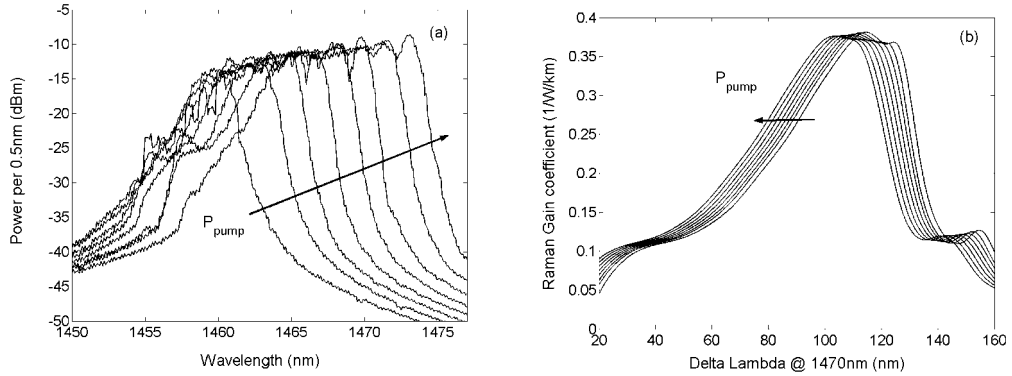

Fig. 7 Measured spectrum of Raman laser diode at 1470 nm for eight pump currents (100 - 800 mA) (a); and modified Raman gain coefficient accounting for the spectral shape of the laser diode (b).

Figure 8 compares the optimized Raman gains assuming monochromatic and broadband sources, and lists the corresponding pump powers. For both cases, a maximum deviation from the target gain of less then 0.2 dB could be achieved. However, note that the pump power levels found for each case differ dramatically from each other. When considering wavelength-stabilized pump sources this effect is not as significant as depicted in Figure 8. However, the power-related spectral broadening of the pumps flattens the effective Raman gain shape g_R^b, which could be advantageously in multi-pump amplifier designs.

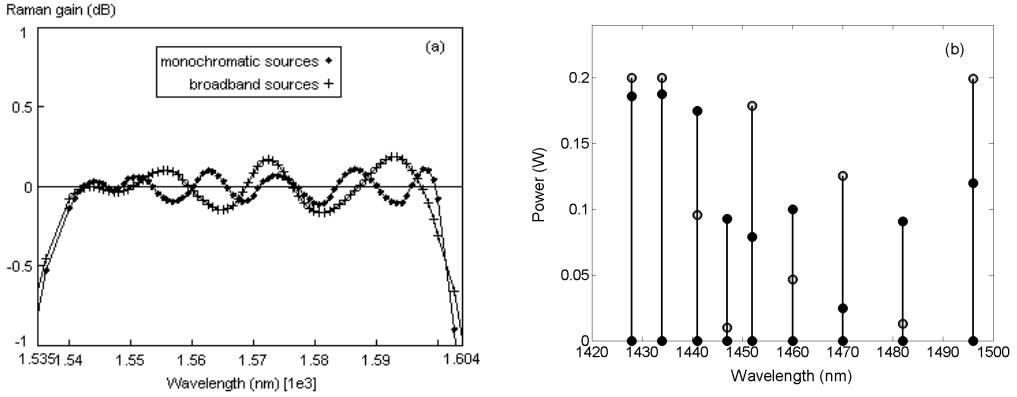

Fig. 8 Optimized Raman gain (a), and corresponding pump power values for monochromatic (filled) and broadband (open) sources (b).

Conclusions

We have developed a method for Raman gain optimization. It considers realistic component characteristics and power constraints while accounting for all Raman and other power-related propagation effects. We have presented results of multi-pump optimization over a heterogeneous fiber span utilizing our proposed technique. We presented optimization results demonstrating the importance of considering Rayleigh and Brillouin scattering. We found that SBS induces a strongly tilted increase of double Rayleigh distortions, which can limit the amplifier performance. We have demonstrated that the power-related variations of broadband Raman pump sources may lead to significant gain variations, and thus, must be considered in the optimization algorithm.

This work was partly supported by Federal Ministry of Education and Research, Germany (01BP268, 01BP267).

References

[1] H. Kidorf, K. Rottwitt, M. Nissov, M. Ma, and E. Rabarijaona, "Pump interactions in a 100-nm bandwidth Raman amplifier," *IEEE Photon. Technol. Lett.*, vol. 11, pp. 530–532, 1999.

[2] S. Namiki, and Y. Emori, "Ultrabroad-band Raman amplifiers pumped and gain-equalized by Wavelength-Division-Multiplexed high-power laser diodes," *IEEE J. Select. Topics Quantum Electron.*, vol. 7, pp. 3–16, 2001.

[3] A.R. Grant, "Calculating the Raman pump distribution to achieve minimum gain ripple," *IEEE J. Quantum Electron.*, vol. 38, pp. 1503–1509, 2002.

[4] V. E. Perlin, and H. G. Wintful, "On distributed Raman amplification for ultrabroad-band long-haul WDM systems," *J. Lightwave Technol.*, vol. 20, pp. 409–416, 2002.
[5] I. Poloyko, A. Khilo, E. Myslivets, V. Volkov, I. Koltchanov, A. Richter, and A. Lowery, "Photonic design automation of Raman-amplified systems," NFOEC 2003 Proceedings, pp. 192-201, Orlando, FL, September 7–11, 2003.
[6] F. Liu, J. Bennike, S. Dey, C. Rasmussen, B. Mikkelsen, P. Mamyshev, D. Gapontsev, and V. Ivshin "1.6 Tbit/s (40x42.7Gbits/s) transmission over 3600 km UltraWave^{TM} fiber with all-Raman amplified 100 km terrestrial spans using ETDM transmitter and receiver" OFC 2002 Proceedings, postdeadline paper FC7-1, Anaheim, CA March 17-22 2002.
[7] P. B. Hansen, L. Eskildsen, A. J. Stentz, T. A. Strasser, J. Judkins, J. J. DeMarco, R. Pedrazzani, and D. J. DiGiovanni, "Rayleigh scattering limitations in distributed Raman pre-amplifiers," *IEEE Photon. Technol. Lett.*, vol. 10, pp. 159–161, 1998.
[8] R.-J. Essiambre, P. Winzer, J. Bromage, and C. H. Kim, "Design of bidirectionally pumped fiber amplifiers generating double Rayleigh backscattering," *IEEE Photon. Technol. Lett.*, vol. 14, pp. 914–916, 2002.
[9] T. Okuno, and M. Nishimura, "Effects of stimulated Raman amplification in optical fibre on stimulated Brillouin scattering threshold power," *Electron. Lett.*, vol. 38, pp. 14–16, 2002.
[10] M. Mehendale, A. Kobyakov, M. Vasilyev, S. Tsuda, and A. F. Evans, "Effect of Raman amplification on stimulated Brillouin scattering threshold in dispersion compensating fibres," *Electron. Lett.*, vol. 38, pp. 268–269, 2002.
[11] C.R.S. Fludger, V. Handerek, and R. J. Mears, "Fundamental noise limit in broadband Raman amplifiers," OFC 2001 Proceedings, Paper MA5, Anaheim, CA, March 17–22, 2001.
[12] Corning Inc., *Corning SMF-28 Optical Fiber Product Information*, PI1036, Corning, NY, August, 2002.
[13] N.R. Newbury, "Raman gain: pump-wavelength dependence in single-mode fiber", *Optics Letters*, vol. 27, pp. 1232-1234, 2002.